Contents available at **PubMed**
www.aidsreviews.com

PERMANYER

AIDS Rev. 2021;23:167-185

A systematic review of magnetic resonance imaging studies in perinatally HIV-infected individuals

Manuela Martín-Bejarano[1], Beatriz Ruiz-Saez[2], Ana Martinez-de-Aragón[3], Helena Melero[4], Berta Zamora[5], Norberto A. Malpica[4], Jose T. Ramos[6], and Maria I. Gonzalez-Tomé[7]*

[1]Department of Paediatrics, Fundación de Investigación Biomédica Hospital Clínico San Carlos, Cohorte Nacional de VIH pediátrica de la RED RIS (CoRISpe); [2]Molecular Immunobiology Laboratory, HIV Spanish Biobank, Hospital Gregorio Marañón; [3]Radiology Department, Hospital Universitario 12 de Octubre; [4]Laboratorio de Análisis de Imagen Médica y Biometría (LAIMBIO), Universidad Rey Juan Carlos; [5]Paediatric Neuropsychology Department, Hospital Universitario 12 De Octubre; [6]Paediatric Infectious Diseases Department, Hospital Clínico San Carlos and Translational Research Network in Pediatric Infectious Diseases (RITIP); [7]Paediatric Infectious Diseases Department, Hospital Universitario 12 De Octubre and NeuroCoRISpe Project, included in CoRIspe (Spanish National Cohort of Paediatric HIV). Madrid, Spain

Abstract

Over the past few years, neuroimaging studies have been performed in young adults with perinatally acquired HIV (PHIV) to study the impact of HIV infection on the central nervous system (CNS), but no recent reviews have been published. This review aims to identify brain areas where PHIV seems to have greater impact taking into account demographic, behavioral, and clinical characteristics in PHIV infected patients. For this purpose, PubMed and Medline searches were carried out which included studies from 2010 to April 2020. We performed a systematic review and included 26 articles using structural (brain morphometry and diffusion tensor imaging) and functional magnetic resonance imaging methods involving 1182 PHIV-infected participants. Ample evidence has been provided of HIV effects on underlying brain structure. However, information recorded in the studies is commonly incomplete and results sometimes contradictory. In addition to future improvements and dissemination of tools for the developing brain MRI processing and analysis, the inclusion of data related to HIV infection itself (including clinical and immunovirological characteristics as well as detailed information about antiretroviral treatment such as age at ART initiation) may be of vital importance to the better understanding of the impact of the disease on CNS.

Key words

HIV/AIDS. Perinatal. Young adults. Magnetic resonance imaging. Neuroimaging.

Introduction

Despite continuing progress in stopping new HIV infections among children, there are 1.8 million children living with HIV, and approximately 160,000 children became infected in 2018[1]. Neurological complications such as encephalopathy associated with HIV (HIVE) in patients perinatally infected (PHIV) were very common in the pre-antiretroviral therapy (ART) era. The incidence of such complications has been significantly reduced in children with the introduction of combined ART (cART); frequent subtle cognitive or behavioral deficits continue to be present[2].

Correspondence to:
*Manuela Martín-Bejarano
E-mail: manuelamartinbg@gmail.com

Received in original form: 03-08-2020
Accepted in final form: 21-02-2021
DOI: 10.24875/AIDSRev.20000088

Individuals who have been diagnosed with PHIV infection may suffer lifelong difficulties, mostly due to neuropsychiatric or cognitive disorders, including deficits in executive functioning (EF), attention, and processing speed (PS)[3-6].

The mechanisms are still unclear, although different non-exclusive factors that could be implicated in persistent central nervous system (CNS) damage have been proposed: presence of HIV-1 RNA in the CNS compartment, toxicities of the cART and/or persistent low-level inflammation in the CNS[7]. This takes on special importance in PHIV infected patients, since the viral CNS invasion occurs within the 1st weeks of life[8].

On the other hand, cART has completely modified the course of HIV infection to a chronic disease in which life expectancy is similar to the HIV negative population[9]. The initiation of cART in infancy and early childhood probably has a direct effect on the child's maturing CNS.

For this reason, several studies have been performed over the past few years to attempt to identify the impact of HIV severity in the CNS on this population group. For instance, neuroimaging studies have contributed to the diagnosis of CNS disorders in PHIV patients, and advances have significantly helped to define the neurological manifestations of HIV infection since the onset of the AIDS pandemic. One of the most relevant tools is magnetic resonance imaging (MRI), a non-invasive neuroimaging technique that allows high-resolution anatomical images of the brain *in vivo* (structural MRI) to be obtained and the observation of brain activity (functional MRI). The quantification of T1-weighted structural data provides relevant measures of brain volume (grey matter, white matter, and cerebrospinal fluid [CSF]; regional volume estimation; and voxel-based morphometry [VBM]) and cortical thickness, whereas Diffusion-Weighted Imaging (DWI) provides measures of fractional anisotropy (FA) and mean diffusivity (MD). The combination of these varied structural measures allows for estimation of the impact of the disorder on the integrity of brain tissue. In addition, functional MRI (fMRI) characterizes brain activity based on the changes that occur in blood flow, volume, and oxygenation (Blood-Oxygen-Level Dependent signal or BOLD signal)[10]. This enables the observation of the functional networks involved in various cognitive tasks (task-based fMRI[11], as well as networks that remain active at rest resting-state fMRI or rs-fMRI[12]). This functional information is essential to understand the cognitive impact of PHIV infection even in the absence of detectable structural alterations.

The first goal of this article is to review recent neuroimaging research findings in patients with PHIV. Specifically, we aim to identify brain areas where PHIV seems to have greater impact taking into account demographic, behavioral, and clinical characteristics in PHIV infected patients. Two MRI techniques have been used in this study: structural (MRI volumetrics and diffusion tensor imaging [DTI]) and functional (fMRI). Other neuroimaging modalities such as magnetic resonance spectroscopy or positron emission tomography have also been used to study this population but have not been evaluated in this systematic review. Single photon emission computed tomography studies do not appear to have been carried out in the PHIV population.

Method

Literature search

The databases searched were PubMed and Medline revealing articles that describe studies from 2010 to April 2020 that have used structural and fMRI measures to build our knowledge of PHIV-associated CNS alterations. Please see Supplemental Material (S1) for an in-depth description of the keywords searched in each neuroimaging technique described.

Study selection criteria

Three qualified researchers systematically evaluated the keywords, titles, and abstracts associated with each individual article to determine those papers that may have met the inclusion and exclusion criteria. If there was confusion or ambiguity regarding an article, it was reviewed independently by the other coauthors and rejected or retained based on the consensus of the research team. Please see figure 1 for an overview of the study selection.

Results

The results of the current review are presented in sections, with two sections accounting for structural (DTI, volume, and cortical thickness) and functional neuroimaging methods (fMRI). For all studies a descriptive table with socio-demographic, cognitive and psychiatric data (see Supplementary Material S2) and medical features of the clinical sample (Table 1) were devised. For each part, two tables (Table 2 for structural neuroimaging and Table 3 for functional neuroimaging) are presented to include information regarding the methods used in each study and the major findings.

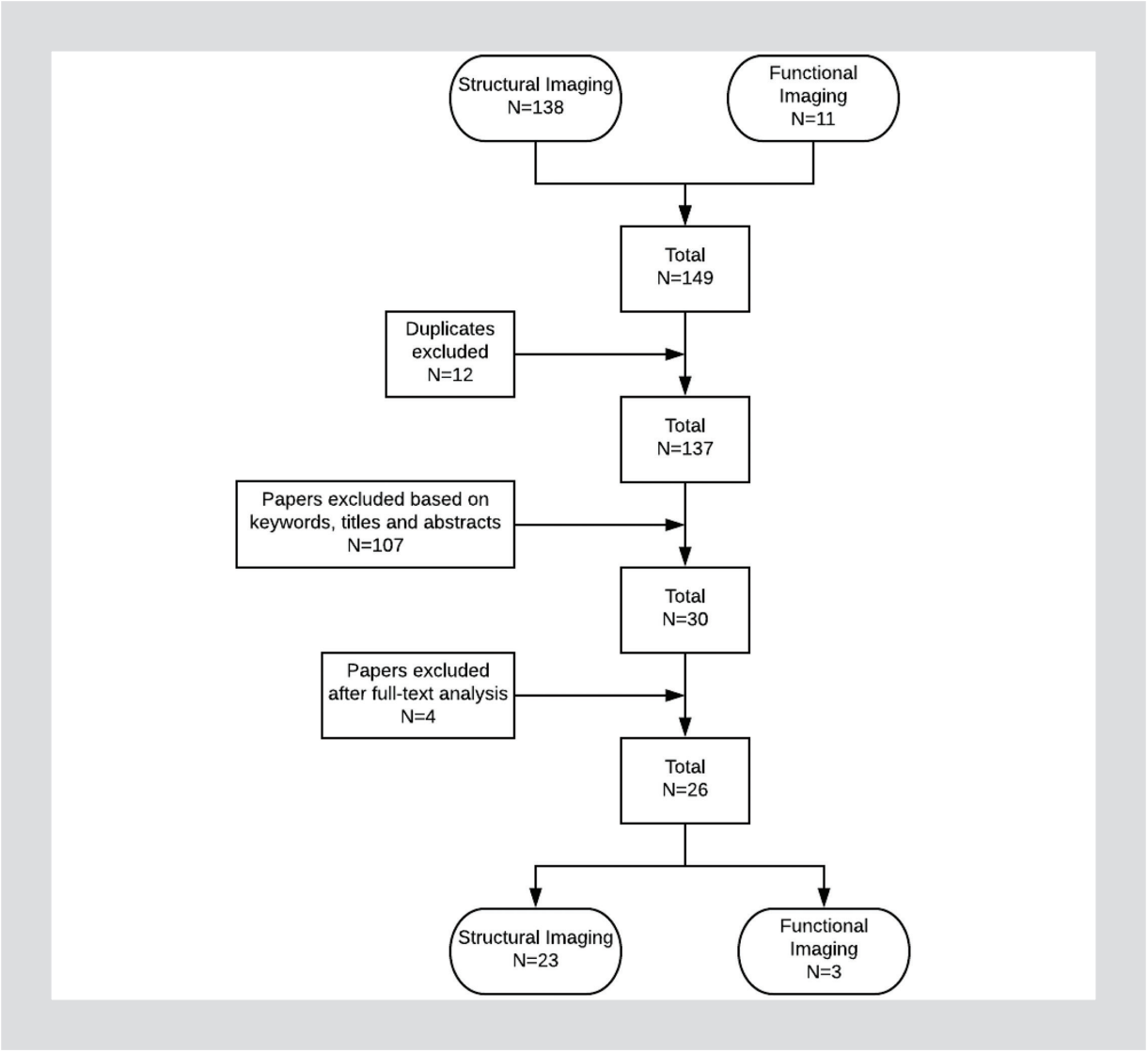

Figure 1. *Literature search flow chart.*

Demographic and behavioral characteristics of the studies selected population

The selected types of neuroimaging studies done on PHIV patients have included 1182 participants[2,13-36]. They have been performed predominantly on sub-Saharan African patients, with seven patients from the Asian population and four Americans. All except four studies have included an HIV negative control group, 50% matched by age (n = 13), 38% by sex (n = 10), and 11% by ethnicity (n = 3). Only two studies matched by years of education and one by socioeconomic status. Fifty percent (n = 13) of the studies have described the education level. Regarding the neuropsychological evaluation, seven papers did not consider cognitive status, and three describe it using screening tools. Among those that used neuropsychological instruments, the main focus with regard to cognitive domains were IQ, PS and EF, with a significant presence of working memory measures included in this last domain.

Only one of the studies included a psychiatric evaluation of the participants, although 27% (n = 7) of the studies referenced psychiatric disorders as exclusion criteria (please see S2).

Clinical measures

The PHIV clinical characteristics that have been recorded and associated with the neuroimaging

Table 1. HIV disease and treatment characteristic

Study	Age at HIV diagnosis (y)	CDC, n (%)	Encephalopathy, n (%)	CD4 Nadir (cells/mm^3, %)	Most recent CD4 at MRI (cells/mm^3, %)	Undetectable viral load, n (%)	HIV on cART, n (%)	Age at cART initiation (years)	Time on cART (years)
Ackermann et al., 2016[13]	NA	NA	NA	NA	cells/mm^3: 1128 (471)	34 (87)	36 (92)	Early cART 0.15 (0.03) Late cART 0.7 (0.3)	NA
Andronikou et al., 2014[15]	NA	NA	0 (0)	cells/mm: 1099 (823-1639) %: 21.4 (16.6-25.6)	cells/mm: 1403 (1026-1766) %: 33.9 (23.9-40.2)	NA	33 (100)	NA	0.29 (0.12)
Andronikou et al., 2015[14]	NA	NA	NA	NA	NA	NA	33 (100)	NA	NA
Cohen et al., 2016[8]	1.2 (0.6-4.9)	N: 4 (13) A: 5 (16) B: 13 (42) C: 9 (29)	2 (8)	Z-score: −0.7 (−1.5-0.4)	cells/mm^3: 800 (590-1.030)	27 (87)	28 (90)	2.2 (0.9-5.2)	11.8 (7.7-14.5)
Herting et al., 2015[16]	NA	NA	2 (6.4)	%: 17 +− 9.5	NA	NA	NA	NA	NA
Hoare et al., 2012[17]	NA	C: 0 (0)	0 (0)	NA	cells/mm^3: 585	11 (91)	0 (0)	-	-
Hoare et al., 2015[18]	NA	NA	NA	NA	NA	NA	NA	NA	NA
Hoare et al., 2015[2]	NA	NA	14 (18.7%)	NA	cells/mm^3: Encephalopathy 1061 ± 464.72 HIV on cART: 1013 ± 552.84 HIV ART naive 615 ± 210	NA	55 (73)	NA	NA
Hoare et al., 2018[19]	NA	NA	NA	NA	cells/mm: 955.12 (587.75)	174 (85)	204 (100%)	3.41	7.18 (2.46)
Hoare et al., 2019[20]	NA	NA	NA	NA	Age of initiation ART < 2 years cells/mm 872.3 (414.54) Age of initiation ART > 2 years cells/mm 989.7 (457.75)	NA	100%	Age of initiation ART < 2 years 1.05 (0.54) Age of initiation ART > 2 years 4.98 (2.41)	Age of initiation ART < 2 years 9.44 (0.73) Age of initiation ART > 2 years 5.75 (2.38)

(Continues)

Table 1. HIV disease and treatment characteristic *(Continued)*

Study	Age at HIV diagnosis (y)	CDC, n (%)	Encephalopathy, n (%)	CD4 Nadir (cells/mm^3, %)	Most recent CD4 at MRI (cells/mm^3, %)	Undetectable viral load, n (%)	HIV on cART, n (%)	Age at cART initiation (years)	Time on cART (years)
Jankiewicz et al., 2017[21]	NA	A: 6 (9) B: 10 (16) C: 49 (75)	8 (12)	cells/mm: 1750 (927) %: 32 (10)	cells/mm^3: 1124 (464) %: 37 (6)	62 (95)	65 (100)	Early cART 0.16 (0.03) Late cART 0.66 (0.34)	Late cART 6.57 (0.37)
Los Angeles et al., 2016[22]	NA	NA	NA	%: 16.5 (8.0-23.8)	%: 35.9 (27.6-2.9)	34 (85)	37 (92)	3.5 (1.4-6.3)	NA
Los Angeles et al., 2017[23]	5.7 (2.2, 10.9)	NA	NA	%: 16.5 (8.0-23.8)	%: 35.9 (27.6-42.9)	34 (85)	37 (92)	NA	NA
Li et al., 2015[24]	NA	NA	0 (0)	NA	cells/mm^3: 605.8 (345.0)	15 (100)	15 (100)	9.5 (3.4)	NA
Li et al., 2018[25]	NA	NA	0 (0)	NA	cells/mm^3: 597 (257)	18 (72)	25 (100)	8.5 (3.3)	6.3 (2.9)
Nwosu et al., 2018[26]	NA	A: 9 (15) B: 19 (32) C: 32 (53)	9 (15)	cells/mm^3: 1899 (914) %: 33 (9.4)	cells/mm^3: 1240 (460) %: cART 36 (6.5)	56 (93)	60 (100)	Early cART 0.16 (0.03) Late cART 0.65 (0.32)	Late cART 6.5 (0.36)
Paul et al., 2018[27]	NA	NA	NA	cells/mm^3: 578 (290-946)	NA	34 (67)	36 (71)	NA	34 (33-42)
Randall et al., 2017[28]	NA	NA	NA	NA	cells/mm^3: 1.029 (677) %: 37 (8)	38 (89)	43 (100)	0.35 (0.31)	Late cART 4.6 (0.46)
Sarma et al., 2013[29]	NA	NA	NA	NA	cells/mm^3: 536 (340)	9 (56)	16 (100)	4.6 (4.8)	NA
Sarma et al., 2019[30]	4.3	NA	NA	NA	cells/mm^3: 630.2 ± 307.5	Log viral load < 1.68: 10	14 (100)	4.9 (4.7)	12.9 (5.3)
Toich et al., 2018[31]	NA	NA	NA	NA	cells/mm^3: 1222 ± 400 %: 36 ± 6	27 (100%)	15 (55) 12 (45) on interrupted cART	10 (8-23)	335 ± 40
Uban et al., 2015[32]	NA	C: 9 (25)	NA	%: 16 (9.5)	%: 33.5 (11.5)	34 (85)	NA	NA	NA
Wade et al., 2019[33]	NA	NA		NA	728 (323)	32 (75)	32 (75)	9.39 (3.23)	NA

(Continues)

Table 1. HIV disease and treatment characteristic *(Continued)*

Study	Age at HIV diagnosis (y)	CDC, n (%)	Encephalopathy, n (%)	CD4 Nadir (cells/mm^3, %)	Most recent CD4 at MRI (cells/mm^3, %)	Undetectable viral load, n (%)	HIV on cART, n (%)	Age at cART initiation (years)	Time on cART (years)
Wang et al., 2018[34]	NA	NA	NA	641.75 ± 291.67	NA	NA	13 (100)	NA	6.50 ± 2.89
Yadav et al., 2017[35]	NA	NA	NA	NA	cells/mm^3: 483 (240)	NA	34 (100)	NA	NA
Yu et al., 2019[36]	NA	NA	0 (0)	NA	558.87 (199.89)	16 (100)	16 (100)	NA	NA

*Data are displayed as mean and SD or median and IQR. NA: not available; SD: standard deviation; IQR: interquartile range; ART: antiretroviral therapy; cART: combined ART, CDC: Centers for Disease Control.

Table 2. Summary information of structural neuroimaging data in each study included

Study	Scanner strength, MRI sequence and acquisition parameters	Analysis software	Measures	Statistical analysis/threshold	Major findings
Ackerman et al., 2016[13]	3T DWI: 30 directions, b factor = NA, TR/TE = 9500/86 ms, FOV = NA, slice thickness = NA, number of slices = NA, gap = NA, acquisition matrix = NA, voxel size = 2 × 2 × 2 mm^3 Sagittal MPRAGE: TR/TE = 2530/1.53/3.19/4.86/6.53 ms, TI = 1160 ms, FOV = 224 × 224 mm^2, flip angle = 7°, number of slices = 144, gap = NA, slice thickness = NA, acquisition matrix = NA, voxel size = 1.3 × 1.0 × 1.0 mm^3	FSL	FA, MD, AD, RD	ANOVA and Chi-square tests $p < 0.05$ (NA)	Two clusters were identified in the right CST, where FA was lower in HIV children than in controls, predominantly due to increased RD. CST rather than the CC were predominantly involved. Children on early-interrupted ART had lower FA compared with those receiving continuous treatment
Andronikou et al., 2014[15]	1.5 T Axial T2 weighted: TR/TE = 5460/103 ms, FOV = NA, acquisition matrix = NA, slice thickness = 5 mm, gap = 1.5 mm, number slices = NA Sagittal T1 weighted: TR/TE = 531/14, FOV = NA, acquisition matrix = NA, slice thickness = 5 mm, gap = 1.5 mm, number of slices = NA	SPM	GM WM, TBV (VBM) y CC thickness and length	Pearson and Spearman $p < 0.05$ (NA)	Premotor segment of the CC mean thickness correlated with age. Motor CC maximum thickness correlated significantly with general developmental quotient; CC length correlated with a diagnosis of acquired microcephaly and to CD4 level closest to date of the MRI scan

(Continues)

Table 2. Summary information of structural neuroimaging data in each study included *(Continued)*

Study	Scanner strength, MRI sequence and acquisition parameters	Analysis software	Measures	Statistical analysis/threshold	Major findings
Andronikou et al., 2015[14]	1.5 T Axial T2 weighted: TR/TE = 5460/103 ms, FOV = NA, acquisition matrix = NA, slice thickness = 5 mm, gap = 1.5 mm, number slices = NA Sagittal T1 weighted: TR/TE 531/14, FOV = NA, acquisition matrix = NA, slice thickness = 5 mm, gap 1.5mm, N° slices = NA	SPM	GM WM, TBV (VBM) y CC thickness and length	t or Mann–Whitney tests Pearson correlation and Spearman $p < 0.05$ (NA)	There were no significant differences between HIV infected patients and uninfected controls. Significant correlations included overall CC (mean) and total brain volume; prefrontal CC maximum with WM volume; premotor CC mean with TBV and WM volume, premotor CC maximum with WM volume and sensory CC mean with TBV
Cohen et al., 2016[8]	3.0 T DWI (DTI): 64 directions, b factor = 1000 s/mm^2, TR/TE = 9476/92 ms, FOV = 224 × 224 mm^2, slice thickness = NA, number of slices = NA, acquisition matrix = NA, voxel size = 2 × 2 × 2 mm^3 Sagittal MPRAGE: TR/TE = 7.0/3.18 ms; TI = 900 ms; FOV = 256 × 256 mm^2, flip angle = 9°, number of slices = 180, slice thickness = NA, gap = NA, acquisition matrix = NA, voxel size = NA	FSL	tWM, CGM, tGM FA, MD, RD, AD	t or Mann–Whitney U-test, Chi-square test Multivariable linear regression $p < 0.05$ (NA)	A lower GM and WM volume, more WMH, and a higher WM diffusivity were observed in the cases. Within the HIV-infected children, a poorer clinical, immunologic, and virologic state were negatively associated with volumetric, WMH, and diffusivity markers
Hoare et al., 2012[17]	3T MRI DWI: 30 directions, b factor = 1000 s/mm^2, TR/TE = 8800/88 ms, FOV = NA, slice thickness = NA, number slices = NA, gap = NA, acquisition matrix = NA, voxel size = 1.8 × 1.8 × 2 mm^3	FSL	FA, MD, RD	t-test and Pearson $p < 0.05$, corrected	"Slow progressors" had lower FA, higher MD and RD in the CC, and increased MD in the SLF, compared to controls. A correlation was found between poor performance on a test of EF and a test of attention with CC FA, and a test of EF with lowered FA in the SLF
Hoare et al., 2015[18]	3T DWI (DTI): 30 directions, b factor = 1000 s/mm^2, TR/TE = 8800/88 ms, FOV = 220, slice thickness = NA, number of slices = NA, gap = 0, acquisition matrix = NA, voxel size = 1.8 × 1.8 × 2 mm^3	FSL	FA, MD, RD, AD	Multiple regression model $p < 0.05$ (NA)	Decreased FA was associated with being on second-line cART, low hemoglobin, and younger age. Children with increased MD, were younger, had reduced albumin and hemoglobin, and increased VL. Decreased AD was associated with increased VL and total protein, decreased albumin and hemoglobin, younger age, poorer fronto-striatal cognition, and being on second-line cART. Increased RD was associated with younger age, low current CD4 count, low albumin and hemoglobin, and higher VL and total protein

(Continues)

Table 2. Summary information of structural neuroimaging data in each study included *(Continued)*

Study	Scanner strength, MRI sequence and acquisition parameters	Analysis software	Measures	Statistical analysis/threshold	Major findings
Hoare et al., 2015[2]	3T DWI (DTI): 30 directions, b factor = 1000 s/mm^2, TR/TE = 8800/88 ms, FOV = 220 mm, acquisition matrix = NA, slice thickness = NA, number of slices = NA, gap = 0, acquisition matrix = NA, voxel size = 1.8 × 1.8 × 2 mm^3	FSL (TBSS) pipeline	FA, MD, RD, AD	ANCOVA $p < 0.05$ corrected	Results of the ANCOVA examining DTI indices between healthy control and HIV-infected group revealed decreased FA, indicating damaged neuronal microstructure, in the left cerebral peduncle and fornix of the HIV-infected group Within the HIV-infected group, children with HIV encephalopathy had poor WM integrity when compared to ART-treated children without encephalopathy, and there was significant myelin loss in ART-naive children, compared with ART treated children. ART-treated children had significant axonal damage in the CC
Hoare et al., 2018[19]	3T DWI (DTI): 30 directions, b factor = 1000 s/mm^2, TR/TE = 8800/88 ms, FOV = 220, slice thickness = NA, number of slices = 65, NA, gap = 0, acquisition matrix = NA, voxel size = 1.8 × 1.8 × 2 mm^3 MPRAGE: TR/TE = 2530/1.53/3.21/ 4.89/6.57 ms, TI = 1100 ms, FOV = 256 × 256 mm^2, flip angle = 7°, number of slices = 144, slice thickness = 1 mm, acquisition matrix = NA, voxel size = 1.3 × 1.0 × 1 mm^3	FSL (TBSS) pipeline Freesurfer	FA MD tWM, tGM, CT and cortical surface area	GLM Pearson and Spearman $p < 0.05$ corrected	HIV infected adolescents had significant FA decreases, MD increases, and decreases in cerebral GM volumes, cortical surface area and decreased gyrification. WB mean FA was significantly reduced in the HIV-infected group. There were significant correlation coefficients between greater total GM and WM volume with the WASI and the Becks self-concept subscale. Lower WB FA was associated with higher scores on the Becks anger and disruptive behavior subscales. Higher WB MD was associated with apathy
Hoare et al., 2019[20]	3T DWI: 30 directions, b factor = 1000 s/mm^2, TR/TE = 8800/88 ms, FOV = 220 mm, slice thickness = NA, number of slices = 65, gap = 0, acquisition matrix = NA, voxel size = 1.8 × 1.8 × 2 mm^3 MPRAGE: TR/TE = 2530/1.53/3.21/ 4.86/6.57 ms, TI = 1100 ms, FOV = 256 × 256 mm, flip angle = 7°, number of slices = 144, gap = NA, slice thickness = 1 mm, acquisition matrix = NA, voxel size = 1.3 × 1.0 mm^3	FSL (TBSS) pipeline	FA, MD, RD, AD	ANOVA t-test $p < 0.05$ (NA)	There was a trend towards attention and WM being poorer in the group who initiated ART > 2 years. FA was lower in the > 2-year group in the superior CR, and the external capsule. MD was higher in the > 2-year group in the cerebral peduncle, the superior CR, and the SFOF. RD was higher in the > 2-year group in the superior CR, the cerebral peduncle, and the SFOF. However, the higher AD in the > 2-year group in the superior CR was not in the expected direction

(Continues)

Table 2. Summary information of structural neuroimaging data in each study included *(Continued)*

Study	Scanner strength, MRI sequence and acquisition parameters	Analysis software	Measures	Statistical analysis/threshold	Major findings
Jankiewicz et al., 2017[21]	3T DWI: 30 directions, b factor = 1000 s/mm^2, TR/TE = 10000/86 ms, FOV = 224 × 224 × 144 mm^3, slice thickness = NA, number of slices = NA, gap = NA, acquisition matrix = 112 × 112 × 72, voxel size = 2 × 2 × 2 mm^3. MPRAGE: TR/TE = 2530/1.53/3.19/4.86/6.53 ms, TI = 1160 ms, FOV = 224 × 224 x 144 mm, flip angle = 7°, number of slices = NA, gap = 0, slice thickness = NA, acquisition matrix = NA, voxel size = 1.3 × 1.0 × 1.0 mm^3	TORTOISE FSL general linear model	FA, MD, RD, AD	General linear model (GLM) $p < 0.05$ (NA)	At 7 years, we found two regions in the left IFOF and left ILF with lower FA in HIV+ children compared to controls. Higher MD was observed in a similar region in the IFOF, albeit bilaterally, as well as multiple clusters bilaterally in the superior CR, the anterior thalamic radiation and the right forceps minor. Unlike at 5 years, we found no impact on WM of ART initiation. In HEU children, we found a cluster in the right posterior CR with higher FA compared to HU children, while bilateral regions in the CST demonstrated reduced MD
Los Angeles et al., 2016[22]	3T Sagittal MPRAGE: TR/TE = 2170/4.37 ms, TI = 1100 ms, FOV = 256 × 256 mm, flip angle = 7°, number of slices = 144, gap: NA, slice thickness = NA, acquisition matrix = 256 × 256 × 160, voxel size = 1 × 1 × 1.2 mm^3	Freesurfer	Surface-based shape	Pearson GLM $p < 0.05$ corrected	Negative correlations between shape deformation and peak HIV VL were found in clusters in the caudate tail, globus pallidus, lateral putamen, and anterior and medial thalamus. Positive correlations between shape deformation and nadir CD4% were found in clusters in the medial and posterior thalamus. Inward deformation in caudate and thalamic clusters correlated with worse cognition
Los Angeles et al., 2017[23]	3T Sagittal MPRAGE: TR/TE = 2170/4.37 ms, TI = 1100 ms; FOV = 256 × 256 mm, flip angle = 7°, number of slices = NA, gap = NA, slice thickness = NA, acquisition matrix = NA, voxel size = 1 × 1 × 1.2 mm^3	Freesurfer	Total and regional GM brain volumes	Spearman, t-test, Pearson linear regression models, GLM $p < 0.05$ (NA)	PHIV youth had smaller total and regional GM volumes than HUE and uninfected youth, with smallest volumes seen among PHIV youth with higher past peak VL and recent unsuppressed VL. In PHIV youth, worse cognitive performance correlated with smaller volumes. Among PHIV youth, smaller volumes were also linked to substance use
Li et al., 2015[24]	3T DWI: 20 directions, b factor = 1000 s/mm^2, TR/TE = 6000/87 ms, FOV = 240 × 240 mm, slice thickness = 3 mm, number of slices = NA, gap = NA, acquisition matrix = 128 × 128 zero filed to 256 × 256, voxel size = NA	FSL	FA, MD, RD, AD	Multiple linear regression analysis 1-way analysis of covariance $p < 0.05$, uncorrected	Relative to HIV-negative controls, HIV-positive adolescents demonstrated significantly reduced FA in the CC, superior and posterior CR, frontal and parietal WM, pre-/post-central gyrus, and SLF. In the affected regions, FA reductions were caused by an increase in RD, and no changes were observed in AD. Moreover, FA values in the bilateral frontal WM were negatively correlated with the duration of HAART and were positively associated with the age at onset of HAART

(Continues)

Table 2. Summary information of structural neuroimaging data in each study included *(Continued)*

Study	Scanner strength, MRI sequence and acquisition parameters	Analysis software	Measures	Statistical analysis/threshold	Major findings
Li et al., 2018[25]	3T Axial MPRAGE: TR/TE = 1900/2.1 ms, TI = 900 ms, FOV = NA, flip angle = 9°; number of slices = 160, gap = NA, slice thickness = 1 mm; acquisition matrix = 320 × 320, voxel size = 1 × 1 mm	SPM12	VBM and structural network analysis (global and regional properties)	t-test, Chi-square test $p < 0.05$, corrected	GM losses were pronounced in ACC, right pallidum, right occipital lobe, inferior parietal lobe, and bilateral cerebellum crus. The global brain network measures were not significantly different between groups; however, the nodal alterations were most pronounced in frontal, temporal, basal ganglia, cerebellum, and temporal lobes. Brain hubs in the HIV-infected subjects increased in number and tended to shift to sensorimotor and temporal areas. In the HIV-infected subjects, decreased GMVs in ACC and bilateral cerebellum were related to lower MMSE scores; the CD4 counts were positively related to the GMVs in ACC and sensorimotor areas
Nwosu et al., 2018[26]	3T MPRAGE: TR/TE = 2530/1.53/3.19/4.86/6.53 ms, TI = 1160 ms, FOV = NA, flip angle = NA, number of slices = 144, gap = NA, slice thickness = NA, acquisition matrix = NA, voxel size = 1.3 × 1.0 × 1.0 mm^3.	Freesurfer	gyrification, regional and total brain volumes	t-test, Chi-square test Linear regression $p < 0.05$	HIV+ children showed reduced gyrification compared to controls in bilateral medial parietal regions, as well as reduced volumes of the right Pu, left hippocampus, and global WM and GM and thicker cortex in small lateral occipital region. Earlier ART initiation was associated with lower gyrification and thicker cortex in medial frontal regions. Early ART appears to preserve CT and volumes of certain brain structures, HIV infection is associated with reduced gyrification in the parietal cortex, and lower Pu and hippocampus volumes
Paul et al., 2018[27]	1.5T MRI Axial 3D SPGR: TR/TE = 11.2/minimum ms, TI = NA, FOV = mm, flip angle = 7°, number of slices = , gap = NA, slice thickness = 1.0mm, acquisition matrix = 256 × 256, voxel size = NA	FSL Freesurfer	caudate, Pu, GP, amygdala, NA, hippocampus, total WM, GM, cortical GM	Chi-square test or Fisher's exact tests and independent t-tests, Linear regression Factor analysis $p < 0.05$ (NA)	HIV- infected children exhibited larger volumes of the caudate, NA, total GM, and cortical GM when compared to the controls. Volumetric differences were predominately evident in children under 12 years of age. Neither cognitive performances nor laboratory markers corresponded to brain volumes in the HIV-infected children

(Continues)

Table 2. Summary information of structural neuroimaging data in each study included *(Continued)*

Study	Scanner strength, MRI sequence and acquisition parameters	Analysis software	Measures	Statistical analysis/threshold	Major findings
Randall et al., 2017[28]	3T MRI Sagittal MPRAGE: TR/TE = 2530/1.53/3.19/4.86/6.53/ms, TI = 1160 ms, FOV = NA, flip angle = 7°, number of slices = 144, gap = NA, slice thickness = NA, acquisition matrix = NA, voxel size = 1.3 × 1.0 × 1.0 mm^3	MultiTracer+ Freesurfer	Basal ganglia and CC	ANOVA Linear regression Multiple regression $p < 0.05$ (NA)	HIV+ children had significantly larger NA and Pu volumes bilaterally and left GP volumes than controls, whilst CC was smaller. Bilateral Pu was larger in both treatment groups compared to controls, while left GP and bilateral NA were enlarged only in ART-After 12 weeks children. CC was smaller in both treatment groups compared to controls, and smaller in ART-After 12 weeks compared to ART-Before 12 Wks. Within infected children, delayed ART initiation was associated with larger Pu volumes, effects that remained significant when controlling for sex and duration of treatment interruption, and lower CD4/CD8 with larger caudates controlling for sex. Volumetric differences were greater in children who initiated ART after 12 weeks
Sarma et al., 2013[29]	3T MPRAGE: TR/TE = 2200/2.34 ms, TI = 900 ms, FOV = 230 × 230 mm, flip angle = 9°, number of slices = 192, gap = NA, slice thickness: 0.9 mm, acquisition matrix = 320 × 320, voxel size = NA	SPM	global and regional GM, WM, and CSF volumes	ANCOVA; uncorrected threshold, $p = 0.001$, uncorrected	WM atrophy appeared in perinatally HIV-infected youths in brain areas including the bilateral posterior CC, bilateral external capsule, bilateral ventral temporal WM, mid cerebral peduncles, and basal pons over controls. GM volume increase was observed in HIV-infected youths including the left superior frontal gyrus, inferior occipital gyrus, gyrus rectus, right mid cingulum, parahippocampal gyrus, bilateral inferior temporal gyrus, and middle temporal gyrus compared with controls. Global WM and GM volumes did not differ significantly between groups
Sarma et al., 2019[30]	3T Axial DWI: 64 directions, b factor = 700 s/mm^2, TR/TE = 10000/90 ms, FOV = 256 × 256 mm, slice thickness = 2 mm, number of slices = 75, gap = 0, acquisition matrix = 130 × 130, voxel size = NA MPRAGE: TR/TE = 2200/2.2 ms, TI = 900 ms, FOV = 240 × 240 mm, flip angle = 9°, number of slices = 176, gap = NA, slice thickness: 1 mm, acquisition matrix = 256 × 256, voxel size = mm^3	SPM	FA, MD, RD, AD	ANCOVA; uncorrected threshold, $p = 0.001$, uncorrected	Regional increases in FA in the PHIV youths were found in left middle frontal gyrus, right precuneus, right lingual gyrus, and left supramarginal gyrus. Increased MD was found in the right precentral gyrus while decreased MD was found in the WM of the right superior parietal lobule and right inferior temporal gyrus/fusiform gyrus. Regions of increased/decreased RD overlapped with regions of increased/decreased MD. Both increased and decreased AD were found in three to four regions respectively

(Continues)

Table 2. Summary information of structural neuroimaging data in each study included *(Continued)*

Study	Scanner strength, MRI sequence and acquisition parameters	Analysis software	Measures	Statistical analysis/threshold	Major findings
Uban et al., 2015[32]	3 T DWI: 30 directions, b factor = 1000 s/mm2, TR/TE = 172,000/86,000 ms, FOV = NA, slice thickness = 2.5 mm, number of slices = NA, gap = NA, acquisition matrix = 96 × 96, voxel size = NA	FSL	FA, MD, RD, AD	ANOVA Pearson Statistical trends were reported (corrected $p < 0.10$)	WB FA was reduced, but RD and MD were increased in PHIV compared with control youth. Within PHIV youth, more severe past HIV disease was associated with reduced FA of the right IFO and left uncinate tracts; elevated MD of the F minor; and increased streamlines comprising the left ILF. Associations of higher peak VL with lower working memory performance were partly mediated by reductions in right IFO FA levels
Wade et al., 2019[33]	1.5 T Axial 3DSPGR: TR/TE = 11.2/minimum ms, FOV = NA, flip angle = , number of slices = NA, gap = NA, slice thickness: 1 mm, acquisition matrix = 256 × 256, voxel size = isotropic	SPM	Thalamus, Pu, pallidum, amygdala, NA, caudate, hippocampus, subcortical shape	Fixed effects multivariate linear regression analyses Longitudinal models $p < 0.05$ (NA)	The PHIV sample were randomized to initiate cART when CD4 counts were 15–24% or when CD4 < 15%. A pallidal subregion was significantly thinner in children with PHIV. Regional thickness, surface area, and volume of the pallidum were associated with CD4 count in children with PHIV. Longitudinal morphometry was not associated with HIV or cART status or timing, however, the trajectory of the left pallidum volume was positively associated with baseline CD4 count
Yadav et al., 2017[35]	3 T Fast spoiled gradient echo FSPGR: TR/TE = 8.4/3.32 ms, TI = 400, FOV = 240 × 240 mm^2, flip angle = 13°, number of slices = NA, gap = NA, slice thickness = 1 mm, acquisition matrix = 512 × 512, voxel size = NA.	Freesurfer	CT and subcortical volumes	t-test, Chi-square test Pearson $p < 0.05$, corrected	Altered CT, subcortical volumes, and abnormal neuropsychological test scores were observed in pediatric HIV patients. The structural network connectivity analysis depicted lower connection strengths, lower clustering coefficients, and higher path length in pediatric HIV patients than HC. The network between ness and network hubs in corticolimbic regions were distorted in pediatric HIV patients

(Continues)

Table 2. Summary information of structural neuroimaging data in each study included *(Continued)*

Study	Scanner strength, MRI sequence and acquisition parameters	Analysis software	Measures	Statistical analysis/threshold	Major findings
Yu *et* al., 2019[36]	3T Axial MPRAGE: TR/TE = 5000/2.88 ms, TI = 700 ms, FOV = NA, flip angle = 4°, number of slices = 176, gap = NA, slice thickness = 1 mm, acquisition matrix = 256 × 256, voxel size = 1 × 1 mm^2	SPM	VBM (volume change and GMV) and CT	t-test, ANOVA $p < 0.05$, corrected	Cross-sectional studies showed that the GM volume of HIV-infected children was widely reduced in the bilateral frontal, temporal, and insular regions, and cerebellum. Longitudinal studies showed that the GM volume reduction of HIV+ children after 1 year occurs in the advanced functional area of the right prefrontal, parietal lobe and the motor area, cortical thinning of brain regions were sensorimotor cortex and the limbic system. The GM volume of the bilateral cerebellum was positively correlated with the WCST, while the CT of the right dorsolateral prefrontal cortex was negatively correlated with WCST

L: left; R: right; S: superior; i: inferior; a: anterior; p: posterior; FA: fractional anisotropy; RD: radial diffusivity; ART: antiretroviral therapy; HC: healthy controls; CC: ***corpus callosum***; GMDS: Griffiths Mental Development Scores; HAART: highly active ART; CD4: CD4 lymphocyte; HIV-: HIV-exposed uninfected; HIV+: HIV-infected; BVT: brain volume Total; CT: cortical thickness; GM: gray matter; WM: white matter; WMH: white matter hyperintensity; WB: whole brain; CDC: Centers for Disease Control; MD: mean diffusivity; SLF: superior longitudinal fasciculus; HEU: HIV exposed uninfected; HU: HIV unexposed uninfected; IFOF: inferior fronto-occipital fasciculus; CST: corticospinal tract; CR: ***corona radiata***; ATR: anterior thalamic radiation; WMI: Working Memory Index; PSI: Processing Speed Index; CPI: Cognitive Proficiency Index; GP: *globus pallidus*; VL: viral load; LH: left hemisphere; NA: nucleus accumbens; IC Interior capsule; FLAIR: fluid-attenuated inversion recovery; ACC: anterior cingulate cortex; GMV: GM volume; MMSE: Mini-Mental State Examination; SWI: susceptibility-weighted imaging; IFO: inferior fronto-occipital; ILF: left inferior longitudinal fasciculus; HC: healthy control; FWE: Family Wise Error; TFCE: threshold-free cluster enhancement; WCST: Wisconsin Card Sorting Test; GLM: general linear model; MRI: magnetic resonance imaging; AD, axial diffusivity; NA: not available; CST: corticospinal tract; VBM: voxel-based morphometry; TGM: total GM; TWM: total WM; CGM: cortical GM; EF: executive functioning

parameters are quite variable, finding predominantly registration of number of patients on cART (23/26), actual CD4 count (21/26), and percentage of patients with undetectable viral load (18/26). Only ten of the 26 studies (38%) have recorded the number of patients with PHIV encephalopathy, and five of those cited this as an exclusion criterion. Five studies (24%) have taken into account the clinical CDC classification of the participants. Moreover, with relation to early initiation of cART, only five studies included this information, and just three of the 26 studies have recorded age at diagnosis (please see Table 1).

Structural neuroimaging

Description of the methods

Structural imaging analysis can currently differentiate neuronal tissue into grey matter, white matter, and CSF measurements in single subjects and across large populations. These *brain morphometry methods* depend on an excellent contrast between different tissues to define grey matter density, grey matter volume, and the inner and outer surface of the cortex. The development of different automatic processing approaches to brain morphometry analysis includes *VBM, deformation-based morphometry (DBM),* and *surface-based morphometry (SBM).*

VBM is a fully automated technique that aims to estimate local differences in tissue composition, after minimizing gross anatomical differences between individuals[37]. The entire brain or specific regions of interest both in healthy subjects and patient groups can be analyzed using VBM[38,39].

While VBM focuses on the residual image variability after subject image transformation, DBM analyses how much the voxel volumes change during subject image registration to the reference template. Using SBM separate features of grey matter anatomy such as surface area, cortical thickness, curvature and volume can be analyzed. SBM differs from VBM and DBM approaches which ultimately analyze image properties at the level of voxels. Surface based cortical thickness measures have the advantage that they allow for subvoxel precision with thickness values being assigned to individual vertices rather than voxels.

DTI is a non-invasive MRI method. The diffusion properties of water in the brain[40] can be used to estimate the integrity of WM tracts using different variables. FA represents an index of the coherence of the diffusion, the degree of myelination of the fibers and

Table 3. Summary information of functional neuroimaging data in each study included

Study	Scanner strength, MRI sequence and acquisition parameters	Analysis software	Modality	Statistical analysis/threshold	Major findings
Herting et al., 2015[16]	3T RS-fMRI: TR/TE = 2000/30 ms, FOV = 64×64 mm^2, flip angle = 75°, Number slices = 33, gap: 4.99, slice thickness: 4 mm, acquisition matrix = NA, voxel size = NA, volumes = 180. MPRAGE: TR/TE = 2170/4.33 ms, TI = 1100 ms, FOV = NA, flip angle = 7°, Number slices = 192, gap: NA, slice thickness: 1.1 mm, acquisition matrix = 256×256, voxel size = NA.	FSL	rs	t-test, Chi-square tests multiple regressions $p < 0.05$, corrected	Global alterations in DMN within- and between-network connectivity, with significant associations between disease severity and DMN BOLD correlations. Furthermore, patterns of connectivity with the posterior cingulate cortex (PCC, p 0,011) and medial prefrontal cortex (mPFC, p 0.006) that varied as a function of peak HIV RNA were found to predict processing speed ability
Toich et al., 2018[31]	3T RS-fMRI: TR/TE = 2000/30 ms, FOV = 220×220×164 mm^3, flip angle = 77°, number of slices = 33, gap = 1mm, slice thickness: 4 mm, acquisition matrix = NA, voxel size = 3.44×3.44×5 mm^3, volumes = 180 Sagital MPRAGE: TR/TE = 2530/1.53/3.19/4.86/6.53 ms, TI = 1160 ms, FOV = 224×224×144 mm^2, flip angle = 7°, number of slices = NA, gap = NA, slice thickness = NA, acquisition matrix = NA, voxel size = 1.3×1 × 1.3 mm^3.	FSL	rs	Regressions $p < 0.05$, NA	No differences within any ICA-generated RSNs between HIV+ and uninfected children, whole brain connectivity to seeds located at RSN connectivity peaks revealed several loci of FC differences, predominantly from seeds in midline regions (posterior cingulate cortex, paracentral lobule, cuneus, and anterior cingulate). Reduced long-range connectivity and increased short-range connectivity suggest developmental delay. Within the HIV+ children, clinical measures at age 7 years was not associated with FC values in any of the RSNs; however, poor immune health during infancy was associated with localized FC increases in the somatosensory, salience and basal ganglia networks
Wang et al., 2018[34]	3T RS-fMRI: TR/TE = 2000/30 ms, FOV = NA, flip angle = 90°, number of slices = 30, gap = 0; slice thickness = 4.5 mm, acquisition matrix = 64×64, voxel size = mm^3, volumes = 210. MPRAGE: TR/TE = 1900/2.1 ms, TI = 900 ms, FOV = NA, flip angle = 9°, number of slices = 176, gap = NA, slice thickness = 1 mm, acquisition matrix = 256×256, voxel size = NA	SPM	rs	t-test, pearson correlation $p < 0.05$, corrected	Significant differences of ReHo values in PHIV+ adolescents compared to PHIV- controls, the areas with ↑ ReHo values include bilateral precentral/post-central gyrus and right middle temporal pole. And the areas with ↓ ReHo values locate in right putamen/pallidum/insula; left caudate/putamen/insula, right superior temporal pole/insula, right caudate/putamen, bilateral anterior cingulate cortex and left inferior temporal pole. Furthermore, age, cognitive scores and nadir CD4+ T-cell counts did not show any significant correlation with altered ReHo values of brain regions neither in PHIV+ groups nor in PHIV- control groups

DMN: default mode network; BOLD: blood-oxygen-level dependent; PCC: posterior cingulate cortex; mPFC: medial prefrontal cortex; RNA: ribonucleic acid; ICA: independent component analysis; RSNS: resting state networks; WB: whole brain; cART: combination antiretroviral therapy; CD4%: CD4 lymphocyte percentage; RS- MRI: magnetic resonance imaging; fMRI: resting state functional MRI; PHACS: Pediatric HIV/AIDS Cohort Study; PHIV: perinatally acquired HIV; FC: functional connectivity; NA: not available, RSNs: resting state networks; ReHo: regional homogeneity.

the degree of axonal damage[41]. This index is the most commonly reported of DTI measures, however, other indices also offer relevant information regarding WM integrity, such as MD, radial diffusivity (RD), and axial diffusivity (AD). MD is an overall measure of displacement of the water molecules and provides information regarding the magnitude of diffusion. A decrease in FA combined with an increase in MD has been suggested to be an indicator of an alteration of WM[42]. AD and RD are indicators of the integrity of the axon and the integrity of the myelin, respectively[43].

Structural neuroimaging in the PHIV population

A summary of structural neuroimaging studies performed in the PHIV+ population are presented in table 2. Initially, 1.5 T field MRI was used to acquire high resolution T1-weighted images, but 3T has been more commonly used in recent studies. SPM, Freesurfer, and FSL are the most widely used analysis software.

Twelve studies used brain morphometry methods (most of them through VBM approach), nine used DTI and two used both methods. With regard to brain morphometry studies comparing PHIV to healthy controls, most of them show reduced GM volumes, cortical surface area and decreased gyrification in the PHIV group except three[27,28,30] which found larger volumes in the same brain areas. One study did not find differences among groups[14]. There is no consensus as to which brain areas seem to be more affected although basal ganglia were often impacted.

In terms of DTI studies, the four most popular indexes were explored in all of them with one exception which only reported FA and MD. Findings seem to agree on FA reduction in the PHIV group and increase in MD within white matter integrity, but no consensus was found regarding the location of these changes depending on the study. For instance, a significant FA reduction was found by some authors in inferior fronto-occipital fasciculus, inferior longitudinal fasciculus[21], whereas this reduction was found by others in superior longitudinal fasciculus (SLF)[24], corticospinal tract[13], or corpus callosum (CC)[17,24] relative to HIV-negative controls.

The alterations in brain structure within the PHIV+ population was related to a poor immunovirological status, in most of the cases defined by high viral load, delayed ART initiation, and lower CD4 count but results are quite variable across the different studies. In general, early ART appears to partially preserve cortical thickness and volumes of certain brain structures[8,26,28], although some abnormalities in white matter are also present in well controlled patients when compared with HIV negative controls[13]. Some authors found associations between actual CD4 count and regional brain volumes[25,33] or brain connectivity[18] but most of them did not. Nevertheless, only one study[8] included complete data about PHIV disease and treatment as recorded in table 1. In this last case, a poorer clinical, immunologic and virologic state were negatively associated with volumetric, WMH, and diffusivity markers.

Several findings suggest that altered cortical and subcortical structures and regional brain connectivity in pediatric HIV patients may contribute to deficits in their cognitive functions[35]. For example, smaller volumes were associated with worse cognitive performance[8,19,23,35,36] with no consensus in the brain structures that experience these changes. However, Paul et al., 2018[27], found that cognitive performances did not correspond to brain volume changes in PHIV-infected children. Where DTI is concerned, some authors posit that similar performance in neurocognitive domains suggests that neurocognitive tests may not be as sensitive as DTI in detecting brain alterations caused by PHIV infection[20]. It is worth noting that some studies have shown some FA changes are sensitive to cognitive performance. Hoare et al.[17] found a correlation between poor performance on a test of EF and a test of attention with CC FA, and a test of EF with lowered FA in the SLF. Similarly, Uban et al.[32] found associations of higher peak viral load with lower working memory performance were partly mediated by reductions in right IFO FA levels. For MD, a negative association with cognition has been described[8,18]. Only one study reported a decrease in AD related to poorer fronto-striatal cognition (PS, EF, and attention)[2].

In overall terms, these studies suggest structural alterations in the PHIV receiving cART. Most studies have been performed cross sectionally, in small samples and differ in terms of neuroimaging methods. International protocols are needed to assess the impact of PHIV-infection on the brain.

fMRI

Description of the method

fMRI is a neuroimaging method that measures brain activity by detecting changes associated with cerebral

blood flow. The neural activity of the brain is indirectly determined by the BOLD response, which is influenced by different factors including cerebral blood flow, blood volume, and the ratio of deoxyhemoglobin to oxyhemoglobin[44].

Two main designs use the BOLD signal to determine the energy used by brain cells: task-related fMRI and resting-state fMRI. Task-related fMRI measures brain activity while someone performs a task while in the scanner. Cerebral blood flow varies depending on the energy required by neurons during a task, and hence the BOLD hemodynamic response, which indirectly represents a measure of neuronal activity[45].

On the other hand, resting-state fMRI reveals the functional connectivity (FC) between distributed neural networks by identifying regions at which the BOLD signal shows temporal coherence. This design offers information about the activity of the brain while the mind is "at rest" and not engaged in tasks.

Several methods to process resting-state fMRI data have been proposed. These can be placed into two groups: model-dependent and model-free methods.

Model-dependent methods ("seed method") are a way of examining the FC of a particular brain region. It is a method that allows for the correlation of the resting-state time-series of the represented brain region against the time-series of all other regions, resulting in a FC map (fcMap) defining the FC of the predefined brain region[46-48]. This region of interest is typically called *seed*.

In contrast to seed-based methods, model-free methods search general patterns of (unique) connectivity across brain structures. Several model-free methods have been suggested and efficiently applied to resting-state time-series, including principal component analysis (PCA)[49], independent component analysis (ICA)[50-52] and hierarchical[53,54], Laplacian[55], and normalized cut clustering[56]. ICA-based methods are the most frequently used and search for a variety of underlying sources that can explain the resting-state patterns, looking for the presence of spatial sources of resting-state signals that are maximally independent from each other. ICA methods can be applied to whole-brain voxel-wise data and as the temporal signals of the independent resting-state components can be easily chosen for further examination of possible group differences between healthy controls and patients. A potential disadvantage of ICA methods might be that the independent components are usually considered more challenging to understand than seed-dependent fcMaps. This could be because they contain a more complex representation of the data, which could confuse the translation of between-group results to clinical relevance[57].

fMRI in the PHIV population

Table 3 summarizes the only three studies that have used resting-state fMRI in PHIV+. 3 T field MRI was used in all studies. SPM and FSL were the software used for analysis.

Evidence of PHIV-related developmental delay has been provided through resting-state FC[16,31,34], showing that young adults with more advanced PHIV disease severity had a "less mature" default mode network. The same regions seem to be at particular risk of alteration in the PHIV population, specifically the medial prefrontal cortex (mPFC), posterior cingulate cortex (PCC), R lateral parietal and occipital cortices, R middle frontal gyrus, L superior frontal gyrus, as well as inferior frontal gyri, although in different hemispheres[16,31].

Wang et al.[34] evaluate regional homogeneity (ReHo) finding differences in several brain areas when compared to a control group. Toich et al.[31], however, found no group differences when using ICA but did find FC differences in whole brain connectivity to seeds located at resting-state networks connectivity peaks revealed several loci, predominantly in the PCC, paracentral lobule, cuneus, and anterior cingulate).

In terms of immunovirological variables, FC was related to viral load and nadir CD4[16] and actual CD4[31]. Wang et al.[34] found no correlation between ReHo and nadir CD4.

In respect of neuropsychological testing only one study[16] evaluated different cognitive domains. Patterns of connectivity with the PCC and mPFC that varied as a function of peak HIV RNA were found to predict PS ability.

Overall, there is preliminary evidence to suggest alterations in FC at rest[16,31,34] finding the method sufficiently sensitive to detect functional alterations in the PHIV population. Further studies are needed with larger sample sizes, better defined control groups, and longitudinal designs.

Conclusions and future directions

All the reviews of neuroimaging research have provided ample evidence that PHIV also has effects on underlying brain structure. Research into the

mechanisms that cause long-term brain disorders is a promising strategy to prevent them. However, there are still limitations, not least of which neuroimaging research is cost- and labor-intensive, and typical studies of only 20-40 patients may be underpowered. The situation is exacerbated in PHIV studies, where recruitment is often more challenging with large variability in multiple variables that often are not recruited. Some of the parameters that would be determinant in neuroimaging studies are missing, such as socioeconomic and health conditions, quality of life, medial characteristics including cART and age at treatment onset, and age at PHIV diagnosis, CDC classification including encephalopathy, other medical comorbidities, including psychiatric disorders or drug use. Furthermore, important factors such as nutrition are not well controlled in African population studies.

High-quality research can be supported by the funding of larger studies, involving collaboration across multiple research groups. However, in spite of the lack of substantial grant funding, researchers can find innovative ways to maximize research resources and boost power through collaboration[58].

Another limitation is that neuroimaging in general, and PHIV brain imaging in particular, contains incomplete, inconsistent, and sometimes contradictory results. This lack of consistency and the differences in techniques account for the variations in research findings[59]. The neuroimaging community has responded to these challenges by synchronizing protocols and data sharing data. Although limited in number, large scale (> 1000 subjects) MRI datasets of healthy infants are available to the scientific community these have not been used in any of the studies reviewed, despite most of the recruited patients being of brain development age. Future PHIV studies ought to employ matching hardware and scan sequences, allowing for comparisons to normative data. While new PHIV imaging studies may want to focus on more specific hypotheses or on more refined imaging technologies, the PHIV community would benefit considerably by also adopting an open-data approach and harmonizing data collection methods and analytical approaches with these larger neuroimaging efforts.

Although remarkable progress has been made, conducting more accurate research has implications studies require more resources, take longer to run / than longitudinal studies, and often yield more conservative results. Solutions including pre-registration of study protocols[60]; transparent reporting of methods and results to limit false interpretations of chance findings[61,62] together with designing studies with sufficient statistical power[58] could have a beneficial impact. On the other hand, transparency can be facilitated by public registration of study protocols and analysis plans before data are collected. This creates an audit trail and clearly delineates confirmatory tests of a priori hypotheses and *post hoc* explorations of data. Statistics should also be openly reported so that others can use the data for power calculations or meta-analysis. Brain volumes means and standard deviations, as well as effect sizes and confidence intervals, should be routinely reported in addition to test statistics and p values. Some of the studies reviewed here did not report actual p values rather than p </> 0.05 which guards against the temptation for rounding errors[63] and did not specify whether results are expressed at an uncorrected or corrected p value threshold.

In summary, this review still found consistent statistical evidence of reduce grey matter volumes, and cortical surface area, decreased gyrification, reduction on FA, and increase in MD in the PHIV-infected group. Furthermore, preliminary data suggest resting-state fMRI is sensitive to detect functional alterations in this population. We believe that future improvements and dissemination of tools for the developing brain MRI processing and analysis will allow us to better chart and understand the dynamic brain developmental trajectories in infants with PHIV-infection, thus informing early diagnosis and intervention.

The inclusion in these studies of data related to PHIV infection itself including clinical and immunovirological characteristics as well as detailed information about antiretroviral treatment such as age at ART initiation may be of vital importance to better understand the impact of the disease on CNS.

Sources of support

This work was supported by Instituto de Salud Carlos III [FIS 15/00694] which is cofunded by Fondo Europeo de Desarrollo Regional: Una manera de hacer Europa; BRS received a Río Hortega grant (health care post-training contract [CM 16/0022]).

Supplementary data

Supplementary data are available at AIDS Reviews online (http://www.aidsreviews.com/). These data are

provided by the corresponding author and published online for the benefit of the reader. The contents of supplementary data are the sole responsibility of the authors.

References

1. UNAIDS. UNAIDS Data 2019 Available from: https://www.unaids.org/en/resources/documents/2019/2019-UNAIDS-data.
2. Hoare J, Fouche JP, Phillips N, Joska JA, Donald KA, Thomas K, et al. Clinical associations of white matter damage in cART-treated HIV-positive children in South Africa. J Neurovirol. 2015;21:120-8.
3. Koekkoek S, de Sonneville LM, Wolfs TF, Licht R, Geelen SP et al. Neurocognitive function profile in HIV-infected school-age children. Eur J Paediatr Neurol. 2008;12:290-7.
4. Judd A, Le Prevost M, Melvin D, Arenas-Pinto A, Parrott F, Winston A, et al. Cognitive function in young persons with and without perinatal HIV in the AALPHI cohort in England: role of non-HIV-related factors. Clin Infect Dis. 2016;63:1380-87.
5. Nachman S, Chernoff M, Williams P, Hodge J, Heston J, Gadow KD. Human immunodeficiency virus disease severity, psychiatric symptoms, and functional outcomes in perinatally infected youth. Arch Pediatr Adolesc Med. 2012;166:528-35.
6. Smith R, Chernoff M, Williams PL, Malee KM, Sirois PA, Kammerer B, et al. Impact of HIV severity on cognitive and adaptive functioning during childhood and adolescence. Pediatr Infect Dis J. 2012;31:592-8.
7. Masters M, Ances, B. Role of neuroimaging in HIV-associated neurocognitive disorders. Semin Neurol. 2014;34:89-102.
8. Cohen S, Caan MW, Mutsaerts HJ, Scherpbier HJ, Kuijpers TW, Reiss P, et al. Cerebral injury in perinatally HIV-infected children compared to matched healthy controls. Neurology. 2016;86:19-27.
9. Justice AC, Modur SP, Tate JP, Althoff KN, Jacobson LP, Gebo KA, et al. Predictive accuracy of the veterans aging cohort study index for mortality with HIV infection: a North American cross cohort analysis. J Acquir Immune Defic Syndr. 2013;62:149-63.
10. Kwong KK, Belliveau JW, Chesler DA, Goldberg IE, Weisskoff RM, Poncelet BP, et al. Dynamic magnetic resonance imaging of human brain activity during primary sensory stimulation. Proc Natl Acad Sci U S A. 1992;89:5675-9.
11. DeYoe EA, Bandettini P, Neitz J, Miller D, Winans P. Functional magnetic resonance imaging (FMRI) of the human brain. J Neurosci Methods. 1994;54:171-87.
12. Biswal B, Yetkin FZ, Haughton VM, Hyde JS. Functional connectivity in the motor cortex of resting human brain using echo-planar MRI. Magn Reson Med. 1995;34:537-41.
13. Ackermann C, Andronikou S, Saleh MG, Laughton B, Alhamud AA, van der Kouwe A, et al. Early antiretroviral therapy in HIV-infected children is associated with diffuse white matter structural abnormality and corpus callosum sparing. AJNR Am J Neuroradiol. 2016;37:2363-9.
14. Andronikou S, Ackermann C, Laughton B, Cotton M, Tomazos N, Spottiswoode B, et al. Corpus callosum thickness on mid-sagittal MRI as a marker of brain volume: a pilot study in children with HIV-related brain disease and controls. Pediatr Radiol. 2015;45:1016-25.
15. Andronikou S, Ackermann C, Laughton B, Cotton M, Tomazos N, Spottiswoode B, et al. Correlating brain volume and callosal thickness with clinical and laboratory indicators of disease severity in children with HIV-related brain disease. Childs Nerv Syst 2014;30:1549-57.
16. Herting MM, Uban KA, Williams PL, Gautam P, Huo Y, Malee K, et al. Default mode connectivity in youth with perinatally acquired HIV. Medicine (Baltimore). 2015;94:1417.
17. Hoare J, Fouche JP, Spottiswoode B, Donald K, Philipps N, Bezuidenhout H, et al. A diffusion tensor imaging and neurocognitive study of HIV-positive children who are HAART-naïve "slow progressors". J Neurovirol. 2012;18:205-12.
18. Hoare J, Fouche JP, Phillips N, Joska JA, Paul R, Donald KA, et al. White matter micro-structural changes in ART-naive and ART-treated children and adolescents infected with HIV in South Africa. AIDS. 2015;29:1793-801.
19. Hoare J, Fouche JP, Phillips N, Joska JA, Myer L, Zar HJ, et al. Structural brain changes in perinatally HIV-infected young adolescents in South Africa. AIDS. 2018;32:2707-18.
20. Hoare J, Heany SJ, Fouche JP, Phillips N, Joska JA, Myer L, et al. Initiation of antiretroviral therapy after the critical neuronal developmental period of the second postnatal year affects white matter microstructure in adolescents living with HIV. J Neurovirol. 2019;25:254-62.
21. Jankiewicz M, Holmes MJ, Taylor PA, Cotton MF, Laughton B, van der Kouwe AJW, et al. White matter abnormalities in children with HIV infection and exposure. Front Neuroanat. 2017;11:88.
22. Los Angeles CP, Alpert KI, Williams PL, Malee K, Huo Y, Csernansky JG, et al. Deformed subcortical structures are related to past HIV disease severity in youth with perinatally acquired HIV infection. J Pediatric Infect Dis Soc. 2016;5:6-14.
23. Los Angeles CP, Williams PL, Huo Y, Wang SD, Uban KA, Herting MM, et al. Lower total and regional grey matter brain volumes in youth with perinatally-acquired HIV infection: associations with HIV disease severity, substance use, and cognition. Brain Behav Immun. 2017;62:100-9.
24. Li J, Wu G, Wen Z, Zhang J, Lei H, Gui X, et al. White matter development is potentially influenced in adolescents with vertically transmitted HIV infections: a tract-based spatial statistics study. AJNR Am J Neuroradiol. 2015;36:2163-9.
25. Li J, Gao L, Wen Z, Zhang J, Wang P, Tu N. Structural covariance of gray matter volume in HIV vertically infected adolescents. Sci Rep. 2018;8:1182.
26. Nwosu EC, Robertson FC, Holmes MJ, Cotton MF, Dobbels E, Little F, et al. Altered brain morphometry in 7-year-old HIV-infected children on early ART. Metab Brain Dis. 2018;33:523-35.
27. Paul R, Prasitsuebsai W, Jahanshad N, Puthanakit T, Thompson P, Aurpibul L, et al. Structural neuroimaging and neuropsychologic signatures in children with vertically acquired HIV. Pediatr Infect Dis J. 2018;37:662-8.
28. Randall SR, Warton CM, Holmes MJ, Cotton MF, Laughton B, van der Kouwe AJW, et al. Larger subcortical gray matter structures and smaller corpora callosa at age 5 years in HIV infected children on early ART. Front Neuroanat. 2017;11:95.
29. Sarma MK, Keller MA, Macey PM, Michalik DE, Hayes J, Nielsen-Saines K, et al. White matter microstructure among perinatally HIV-infected youth: a diffusion tensor imaging study. J Neurovirol. 2019; 25:313-23.
30. Sarma MK, Nagarajan R, Keller MA, Kumar R, Nielsen-Saines K, Michalik DE, et al. Regional brain gray and white matter changes in perinatally HIV-infected adolescents. Neuroimage Clin. 2013;4:29-34.
31. Toich JT, Taylor PA, Holmes MJ, Gohel S, Cotton MF, Dobbels E, et al. Functional connectivity alterations between networks and associations with infant immune health within networks in HIV infected children on early treatment: a study at 7 years. Front Hum Neurosci. 2018;11:635.
32. Uban KA, Herting MM, Williams PL, Ajmera T, Gautam P, Huo Y, et al. White matter microstructure among youth with perinatally acquired HIV is associated with disease severity. AIDS. 2015;29:1035-44.
33. Wade BS, Valcour VG, Puthanakit T, Saremi A, Gutman BA, Nir TM, et al. Mapping abnormal subcortical neurodevelopment in a cohort of Thai children with HIV. Neuroimage Clin. 2019;23:101810.
34. Wang P, Li J, Wang X, Thapa D, Wu GY. Asymptomatic human immunodeficiency virus vertical transmitted adolescents' brain functional changes: based on resting-state functional magnetic resonance imaging. AIDS Res Hum Retroviruses. 2018;34:699-704.
35. Yadav SK, Gupta RK, Garg RK, Venkatesh V, Gupta PK, Singh AK, et al. Altered structural brain changes and neurocognitive performance in pediatric HIV. Neuroimage Clin. 2017;14:316-22.
36. Yu X, Gao L, Wang H, Yin Z, Fang J, Chen J, et al. Neuroanatomical changes underlying vertical HIV infection in adolescents. Front Immunol. 2019;10:814.
37. Ashburner J, Friston KJ. Voxel-based morphometry--the methods. Neuroimage. 2000;11:805-21.
38. Geva S, Baron JC, Jones PS, Price CJ, Warburton EA. A comparison of VLSM and VBM in a cohort of patients with post-stroke aphasia. Neuroimage Clin. 2012;1:37-47.
39. Rowan A, Vargha-Khadem F, Calamante F, Tournier JD, Kirkham FJ, Chong WK, et al. Cortical abnormalities and language function in young patients with basal ganglia stroke. Neuroimage. 2007;36:431-40.
40. Johnson VE, Stewart W, Smith DH. Axonal pathology in traumatic brain injury. Exp Neurol. 2013;246:35-43.
41. Yang E, Nucifora PG, Melhem ER. Diffusion MR imaging: basic principles. Neuroimaging Clin North Am. 2011;21:1-25.
42. Sundman M, Doraiswamy PM, Morey RA. Neuroimaging assessment of early and late neurobiological sequelae of traumatic brain injury: implications for CTE. Front Neurosci. 2015;9:334.
43. Wheeler-Kingshott CA, Cercignani M. About "axial" and "radial" diffusivities. Magn Reson Med. 2009;61:1255-60.
44. Schleim S, Roiser JP. FMRI in translation: the challenges facing real-word application. Front Hum Neurosci. 2009;3:63.
45. Dickerson BC. Advances in functional magnetic resonance imaging: technology and clinical applications. Neurotherapeutics. 2007;4:360-70.
46. Biswal BB, Van Kylen J, Hyde JS. Simultaneous assessment of flow and BOLD signals in resting-state functional connectivity maps. NMR Biomed. 1997;10:165-70.
47. Cordes D, Haughton VM, Arfanakis K, Wendt GJ, Turski PA, Moritz CH, et al. Mapping functionally related regions of brain with functional connectivity MR imaging. AJNR Am J Neuroradiol. 2000;21:1636-44.
48. Jiang T, He Y, Zang Y, Weng X. Modulation of functional connectivity during the resting state and the motor task. Hum Brain Mapp. 2004;22:63-71.
49. Friston KJ. The disconnection hypothesis. Schizophr Res. 1998;30:115-25.

50. Beckmann CF, DeLuca M, Devlin JT, Smith SM. Investigations into resting-state connectivity using independent component analysis. Philos Trans R Soc Lond B Biol Sci. 2005;360:1001-13.
51. Calhoun VD, Adali T, Pearlson GD, Pekar JJ. A method for making group inferences from functional MRI data using independent component analysis. Hum Brain Mapp. 2001;14:140-51.
52. De Luca M, Beckmann CF, De Stefano N, Matthews PM, Smith SM. FMRI resting state networks define distinct modes of long-distance interactions in the human brain. Neuroimage. 2006;29:1359-67.
53. Cordes D, Haughton V, Carew JD, Arfanakis K, Maravilla K. Hierarchical clustering to measure connectivity in fMRI resting-state data. Magn Reson Imaging. 2002;20:305-17.
54. Salvador R, Suckling J, Coleman MR, Pickard JD, Menon D, Bullmore E. Neurophysiological architecture of functional magnetic resonance images of human brain. Cereb Cortex. 2005;15:1332-42.
55. Thirion B, Dodel S, Poline JB. Detection of signal synchronizations in resting-state fMRI datasets. Neuroimage. 2006;29:321-7.
56. van den Heuvel M, Mandl R, Hulshoff Pol H. Normalized cut group clustering of resting-state FMRI data. PLoS One. 2008;3:2001.
57. Fox MD, Raichle ME. Spontaneous fluctuations in brain activity observed with functional magnetic resonance imaging. Nat Rev Neurosci. 2007;8:700-11.
58. Button KS, Ioannidis JP, Mokrysz C, Nosek BA, Flint J, Robinson ES, et al. Power failure: why small sample size undermines the reliability of neuroscience. Nat Rev Neurosci. 2013;14:365-76.
59. Jovicich J, Marizzoni M, Sala-Llonch R, Bosch B, Bartrés-Faz D, Arnold J, et al. Brain morphometry reproducibility in multi-center 3T MRI studies: a comparison of cross-sectional and longitudinal segmentations. Neuroimage. 2013;83:472-84.
60. Dickersin K, Rennie D. The evolution of trial registries and their use to assess the clinical trial enterprise. JAMA. 2012;307:1861-4.
61. Rennie D. CONSORT revised--improving the reporting of randomized trials. JAMA. 2001;285:2006-7.
62. Simera I, Moher D, Hirst A, Hoey J, Schulz KF, Altman DG. Transparent and accurate reporting increases reliability, utility, and impact of your research: reporting guidelines and the EQUATOR Network. BMC Med. 2010;8:24.
63. John LK, Loewenstein G, Prelec D. Measuring the prevalence of questionable research practices with incentives for truth telling. Psychol Sci. 2012;23:524-32.